

**Crystalline GeTe-based phase-change alloys: Disorder in order**

Milos Krbal, Alexander V. Kolobov,\* Paul Fons, and Junji Tominaga

*Nanodevice Innovation Research Center, National Institute of Advanced Industrial Science and Technology, Tsukuba Central 4, Higashi 1-1-1, Tsukuba, Ibaraki 305-8562, Japan*

S. R. Elliott

*Department of Chemistry, University of Cambridge, Lensfield Road, Cambridge, CB2 1EW United Kingdom*

J. Hegedus

*COMP/Department of Applied Physics, Aalto University School of Science, P.O. Box 11100, FI-00076 Aalto, Finland*

A. Giussani, K. Perumal, and R. Calarco

*Paul-Drude-Institut für Festkörperelektronik, Hausvogteiplatz 5-7, 10117 Berlin, Germany*

T. Matsunaga

*Material & Process Development Center, Panasonic Corporation 3-1-1 Yagumo-Nakamachi, Moriguchi, Osaka 570-8501, Japan*

N. Yamada

*Advanced Technology Research Laboratories, Panasonic Corporation 3-4 Hikari-dai Seika-cho, Kyoto, 619-0237, Japan*

K. Nitta and T. Uruga

*Japan Synchrotron Radiation Research Institute, 1-1-1 Koto, Sayo, Hyogo 679-5198, Japan*

(Received 21 March 2012; revised manuscript received 27 June 2012; published 23 July 2012; corrected 6 August 2012)

Through the combined use of x-ray absorption and scattering experiments and *ab initio* simulations, we demonstrate that the metastable cubic phase of GeTe-based phase-change alloys, e.g.  $\text{Ge}_2\text{Sb}_2\text{Te}_5$ , is significantly more disordered than is generally believed, with a large number of Ge atoms located off octahedral resonantly bonded sites. The stochastic off-octahedral locations of Ge atoms, that are invisible to Bragg diffraction probing the average structure, lead to disruption of the continuous resonance bonding network of the crystalline phase, resulting in localization of charge carriers. It is proposed that the degree of coherency of local rhombohedral displacements, that may be varied, e.g., by doping, can serve as means to control electrical properties of Ge-Sb-Te alloys.

DOI: [10.1103/PhysRevB.86.045212](https://doi.org/10.1103/PhysRevB.86.045212)

PACS number(s): 61.66.-f, 61.05.cj, 71.23.-k

**I. INTRODUCTION**

Tellurium-based alloys, especially those along the GeTe- $\text{Sb}_2\text{Te}_3$  tie-line (GST), are widely used in optical memory devices, such as digital versatile discs (DVDs), and are also among the leading candidates for the next generation of nonvolatile electronic memories.<sup>1</sup> In these materials, information is stored as optical and electrical property contrast arising from structural differences between the crystalline and amorphous phases. Despite significant progress on the application front, many fundamental issues, including the structure of the crystalline phase, pose important challenges.

Early Bragg diffraction studies suggested that at room temperature and above, the device-relevant metastable crystalline phase has the rock-salt structure with Te atoms forming one face-centered cubic sublattice and Ge/Sb and vacancies forming the other. Based on a Rietveld refinement that assumed the cubic structure, rather large values for isotropic thermal factors were reported, especially for Ge atoms, suggesting large atomic displacements from the ideal crystallographic positions.<sup>2</sup> Subsequent extended x-ray absorption fine structure (EXAFS) experiments demonstrated that locally the structure is distorted similarly to the case of the binary GeTe and has subsets of three short (ca. 2.83 Å) and three long

Ge-Te (ca. 3.15 Å) bonds. The obtained mean-square relative displacement values for the crystalline phase were *larger than in the amorphous phase* indicating a very large distribution of the bond lengths.<sup>3</sup>

GeTe-based alloys exhibit a ferroelectric-to-paraelectric transition which has long been believed to be displacive in nature.<sup>4</sup> Recent studies using x-ray absorption fine structure (XAFS) demonstrated that the apparent displacive nature in GeTe is a result of the averaging effect of Bragg diffraction: the subsets of the shorter and longer bonds are preserved across the transition with the displacement direction becoming stochastic, which results in the cubic average structure.<sup>5</sup> This conclusion has been confirmed by a pair-distribution function (PDF) analysis of total scattering where the apparently cubic phase could be well fit by a model with the Ge atom positions distributed among four different sites displaced along the four  $\langle 111 \rangle$  directions as well as their inverse such that the rhombohedral displacement averaged to zero,<sup>6</sup> thereby generating a large isotropic thermal factor.

For the GeTe structure that is locally rhombohedrally distorted so that it appears cubic on average, the coherent domain size should be on the order of a few nanometers. One can roughly estimate the size of coherent domains in the

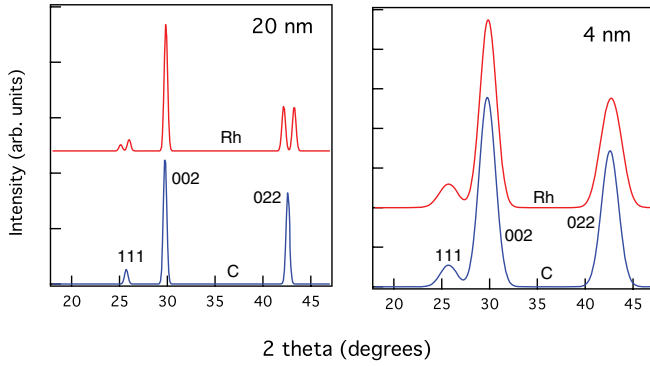


FIG. 1. (Color online) Simulated x-ray powder diffraction patterns ( $\lambda = 1.541 \text{ \AA}$ ) for the low-temperature rhombohedral (Rh) and high-temperature cubic (C) phases of GeTe with different coherence domain sizes (shown in the upper right-hand corner of the corresponding panel). Peaks in the cubic phase are labeled.

high-temperature (locally rhombohedrally distorted but apparently cubic) phase of GeTe by simulating x-ray diffraction spectra. Figure 1 shows the results of such simulations performed using CrystalMaker and CrystalDiffract. For larger coherent domains (20 nm in the left-side panel), the spectra for the rhombohedrally distorted and cubic phases are clearly different with the peaks located at ca.  $26^\circ$  and  $43^\circ$  split in the rhombohedral phase. At the same time, these peaks merge into a single broad peak (with an apparently large isotropic temperature factor) for grain sizes of 4 nm and below (right-side panel); the patterns for the rhombohedrally distorted and cubic phases become essentially identical and apparently cubic. The grain sizes in the real sample can be larger than the coherence domain size.

When additional disorder is introduced, e.g., due to doping (alloying with  $\text{Sb}_2\text{Te}_3$  may be considered as doping from this perspective), the temperature of the ferroelectric-to-paraelectric transition decreases which was interpreted as a doping-induced disordering of the Ge sublattice.<sup>7,8</sup> It should also be noted that the charge carriers in crystalline GST experience Anderson localization that is typically associated with lattice disorder.<sup>9</sup>

Bonding in crystalline phase-change materials is usually described as being resonant<sup>10</sup> with shorter, essentially covalent, bonds and longer resonance bonds formed through the back lobes of the same  $p$  orbitals that are used to form the shorter bonds. Below we demonstrate that stochastic distortions have a drastic effect on the nature of interatomic interactions and consequently on material properties.

The shorter and longer bonds exhibit a strong bonding energy hierarchy and during the amorphization process the longer resonance bonds break with the covalent backbone being preserved.<sup>11</sup> The current consensus is that, in the amorphous phase of Ge, atoms are located on both tetrahedral sites (four essentially equal Ge-Te bonds ca.  $2.61 \text{ \AA}$  long) and on lower coordinated sites with octahedral bonding angles. The latter can be described as being  $3 + n$  coordinated sites<sup>12,13</sup> with three shorter (ca.  $2.75 \text{ \AA}$ ) Ge-Te bonds and additional  $n$  neighbors located at interatomic distances of ca.  $3.10 \text{ \AA}$ . From this perspective, the coordination number of Ge species in the crystalline phase can be described as  $3 + 3$ , i.e., the difference

in bonding between the crystalline and amorphous phases being essentially in the number of “resonantly” interacting Ge-Te pairs. The number of resonantly bonded Te neighbors has a drastic effect on the Ge  $K$ -edge x-ray absorption near-edge structure (XANES) spectra,<sup>12</sup> which can serve to distinguish between the crystalline ( $n = 3$ ) and amorphous ( $n < 3$ ) structures. (XANES is a technique that is suitable to discern local differences in bonding due to its nanometer-order sampling length as well as its sensitivity to higher-order correlations via the angular dependence of multiple scattering.<sup>14</sup>)

In this work, we report on experimental XAFS and total scattering measurements as well as *ab initio* simulations that allow us to propose a consistent nanometer-scale structure for the crystalline phase of GeTe-based phase-change alloys.

## II. EXPERIMENTAL AND SIMULATIONAL DETAILS

Polycrystalline samples were prepared by rf sputtering and subsequent annealing; epitaxial layers used in this work were grown at the Paul Drude Institute on InAs(001) substrates, the growth conditions being described in Ref. 15. XAFS and total scattering measurements were performed at SPring-8 on beamlines BL01B1 and BL02B2, respectively; more details can be found elsewhere.<sup>6</sup> XANES simulations were performed using the procedure described in Ref. 12.

## III. RESULTS AND DISCUSSION

First, we used EXAFS to compare the disorder in the Ge and Te sublattices. Figure 2 shows Fourier-transformed Te  $K$ -edge and Ge  $K$ -edge EXAFS spectra of GeTe and  $\text{Ge}_2\text{Sb}_2\text{Te}_5$ . In the binary material GeTe the second (like-atom) peaks are clearly observed at both the Ge and Te edges. At the same time, in  $\text{Ge}_2\text{Sb}_2\text{Te}_5$ , the second-nearest neighbor peak (for the Ge  $K$  edge) corresponding to Ge-Ge(Sb) correlations at  $4.25 \text{ \AA}$  essentially disappears indicating increased disorder in the Ge(Sb) sublattice. To a first approximation, the structure can be viewed as a superposition of an ordered Te fcc lattice

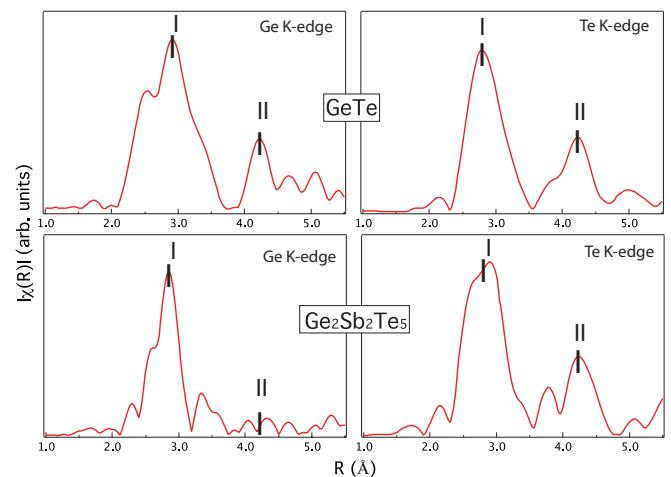


FIG. 2. (Color online) Fourier transformed Ge  $K$ -edge and Te  $K$ -edge EXAFS spectra of (poly)crystalline GeTe and  $\text{Ge}_2\text{Sb}_2\text{Te}_5$  alloys measured at 10 K. Labels “I” and “II” refer to the first- and second-nearest neighbor shells, respectively

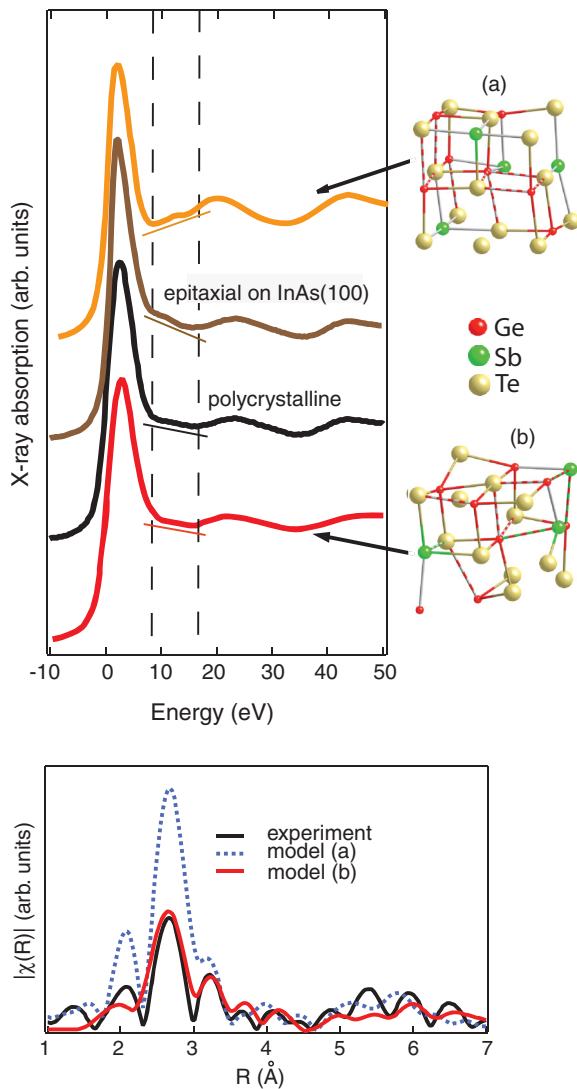


FIG. 3. (Color online) Experimental (at 20 K) and simulated Ge  $K$ -edge XANES (upper panel) and Fourier-transformed EXAFS (lower panel) spectra for the metastable cubic phase of  $\text{Ge}_2\text{Sb}_2\text{Te}_5$ . Simulations were done for two different models (a) and (b) (see text for details).

and a disordered Ge/Sb lattice. A similar result, i.e., increased local disorder, was also observed for GeTe doped with nitrogen and carbon.<sup>8</sup>

We have further performed XANES simulations to investigate the nanometer-range structure of the crystalline phase. Figure 3 (upper panel) shows experimentally measured Ge  $K$ -edge XANES spectra for the crystalline phase of  $\text{Ge}_2\text{Sb}_2\text{Te}_5$  (a polycrystalline film as well as an epitaxial film) together with simulated spectra generated using different models. Model (a) is a relaxed rock-salt structure of  $\text{Ge}_2\text{Sb}_2\text{Te}_5$  (containing 20 Ge atoms) obtained through density-functional-theory simulations.<sup>16</sup> A fragment of such a structure with a Ge atom at the center is shown in the figure. One can immediately see that in the region between the dashed lines, where the slope serves as a fingerprint to distinguish between the crystalline and amorphous phases, both structures yield XANES spectra that are significantly different from the simulated one. This result

is in stark contrast to the case of amorphous  $\text{Ge}_2\text{Sb}_2\text{Te}_5$  where the agreement between experiment and simulations was nearly perfect (see Fig. 3 of Ref. 12) and demonstrates that while the rock-salt model provides an adequate description of the global structure, it fails to describe accurately the short-range order of the crystalline phase of  $\text{Ge}_2\text{Sb}_2\text{Te}_5$ . At the same time, structure (b), obtained by rapidly quenching *in silico* liquid  $\text{Ge}_2\text{Sb}_2\text{Te}_5$ , such that it contains a large number of covalently bonded configurations (a typical fragment with a central Ge atom is shown), gives a near-perfect agreement with experiment. Models (a) and (b) were also used to simulate EXAFS: the experimentally measured spectrum for the crystalline phase is also much better reproduced by the locally disordered structure (Fig. 3, lower panel) which gives further support to our conclusions.

Nonresonantly bonded Ge atoms in GeTe can be of two kinds: (i) Ge atoms at grain boundaries; and (ii) Ge atoms located at boundaries between coherent domains formed as a result of the ferroelectric order-disorder transition. The fact that the spectra for the polycrystalline film that contains numerous grain boundaries and epitaxial films are rather similar and both different from the simulated spectra for the rock-salt structure clearly demonstrates that the disagreement between experiment and simulations does not arise from the presence of grain boundaries.

We believe that this discrepancy is an intrinsic feature of the crystalline phase and arises from the fact that Ge atoms in GeTe (and GeTe-based alloys) are stochastically displaced. Indeed, while the subsets of the shorter and longer bonds with an extended resonance network can exist for the phase [Fig. 4(b)] assuming an ordered *cubic* Te sublattice suggested by the global rock-salt structure, in the case of a *rhombohedrally* distorted Te sublattice phase some of the Ge atoms necessarily become misaligned [Fig. 4(c)]. As has been demonstrated earlier, loss of atomic alignment leads to the destruction of resonance bonds and subsequently the formation of a disordered phase.<sup>11,17</sup> As a result, a fraction of Ge atoms has a local structure similar to that in the amorphous phase, which accounts for the observed slope in region II in the experimental XANES spectrum.

With an increase in temperature, the rhombohedral angle approaches  $90^\circ$  (Fig. 5) as demonstrated by PDF analysis of the total scattering, possibly enabling the formation of a more extended resonance bonding network.

The existence of covalently bonded fragments in the crystalline phase can be explained by the fact that the energy difference between the crystalline and amorphous phases (measured using differential scanning calorimetry) is in the  $\Delta E$  range of 28 to 42 meV/atom.<sup>18</sup> Considering such fragments as defects within the (ideally) resonantly bonded crystal, one can make a simple estimate of the fraction of such defects ( $e^{-\frac{\Delta E}{kT}}$ ); at room temperature one obtains as many as 30% of covalently bonded configurations in the nominally resonantly bonded crystalline phase. Furthermore, the small formation energy implies that their presence in the resonantly bonded crystalline phase is an intrinsic feature of the latter. It is interesting to note that the observation of a significant fraction of Ge atoms located off octahedral sites has recently been reported by high-resolution transmission electron microscopy.<sup>19</sup>

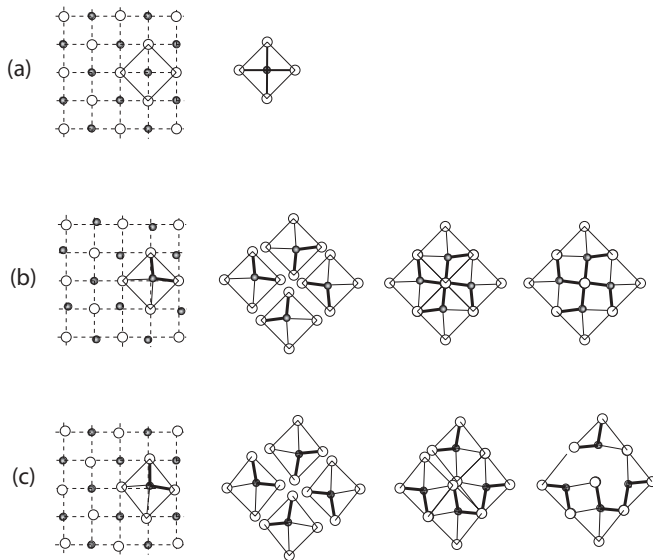


FIG. 4. Schematic two-dimensional illustration of stochastic distortions causing destruction of the continuous resonant-bonding network. When one starts with (a) the perfect rock-salt structure, (b) a cubic phase of GeTe with randomly displaced Ge atoms can be reproduced using a larger unit cell that includes differently distorted Ge atoms preserving the necessary alignment for the formation of a continuous resonant-bonding network. At the same time, for the case of (c) the rhombohedral structure, space cannot be filled with differently oriented rhombohedra resulting in atomic misalignment and subsequent rupture of certain resonant interactions. For simplicity we assume (see Fig. 1) that Ge atoms are randomly displaced within an ordered Te sublattice.

We now address the effect of the presence of off-resonance Ge sites on the electrical properties of phase-change alloys. GeTe (and possibly GST alloys) is a degenerate p-type semiconductor with the top of the valence band formed by  $p$  electrons. It is these  $p$  electrons that determine both bonding and charge transport. In the near-perfect cubic phase all atoms and consequently their  $p$  orbitals are aligned, and

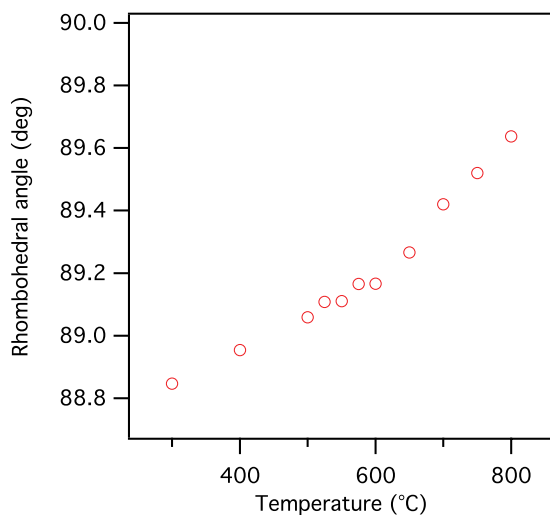


FIG. 5. (Color online) Temperature dependence of the rhombohedral angle in crystalline GeTe obtained from a PDF analysis of the total scattering.

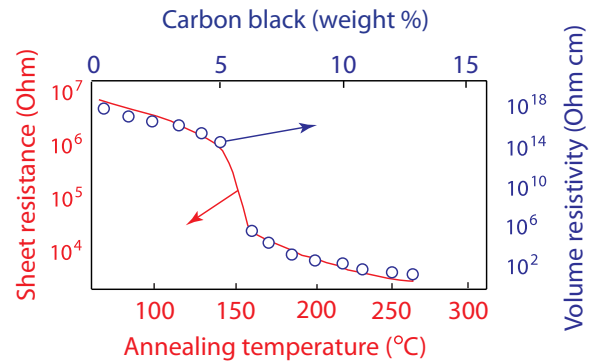


FIG. 6. (Color online) Comparison of the resistivity change in Ge<sub>1</sub>Sb<sub>2</sub>Te<sub>4</sub> upon heating across the crystallization temperature (red line)<sup>9</sup> and in a composite compound of carbon black and high-density polyethylene upon changing the composition across the percolation threshold (blue circles).<sup>21</sup>

the resonant-bonding network extends throughout the crystal, while in the amorphous phase resonance bonding is localized to within several interatomic distances. Consequently, the two phases have very strong property differences, as exemplified by the large changes in quantities, such as optical or conductivity contrast.

Destruction of the continuous resonant network of the crystalline phase, due to the intrinsic structural disorder described above, which can be alternatively described as inclusion of covalently bonded fragments with a more localized bonding nature, has a drastic effect on the properties of the material. We believe that a gradual increase in conductivity during annealing above the crystallization temperature (which follows an abrupt decrease due to crystallization) reported earlier for Ge-Sb-Te alloys and explained in terms of Anderson localization<sup>9</sup> may also be caused by the presence of covalently bonded fragments within the crystalline phase that serve to disrupt the continuity of the resonant-bonding network in a way similar to the vandalized grid description of a percolation process.<sup>20</sup> Indeed, the reported behavior is remarkably similar (see Fig. 6) to the percolation threshold observed in materials that are mixtures of conducting and insulating phases when an abrupt drop in resistivity due to the formation of a continuous percolating current path is followed by a much slower decrease in resistivity due to an increasingly large fraction of the conductive phase.<sup>21</sup> Similarly to the formation of extended conducting phases in heterogeneous mixtures, in phase-change materials, as the temperature is increased, the rhombohedral angle approaches 90° (Fig. 5) enabling the formation of a more extended resonance bonding network [Fig. 4(c) → Fig. 4(b)] with a concomitant increase in conductivity in agreement with experiment.<sup>9</sup>

We suggest that the observed changes in conductivity may be related to postcrystallization ordering of the material. To verify this idea we investigated intermediate-range order structural changes in Ge<sub>2</sub>Sb<sub>2</sub>Te<sub>5</sub> across the crystallization temperature and up to 150 degrees above it with the heating ramp of 0.3 deg/min using XANES measurements. Figure 7 (upper panel) shows the XANES spectra for the Ge<sub>2</sub>Sb<sub>2</sub>Te<sub>5</sub> sample measured at different temperatures. In Fig. 7 (lower panel) we show the fitting results when the experimental XANES spectra were

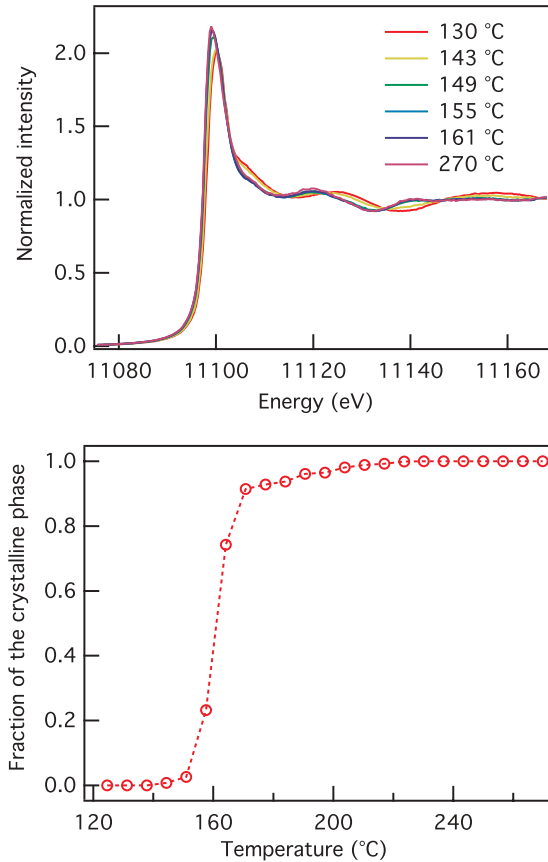


FIG. 7. (Color online) (Upper panel) Temperature evolution of  $\text{Ge}_2\text{Sb}_2\text{Te}_5$  XANES spectra during the crystallization process, and (Lower panel) the amount of the crystalline phase obtained from fitting the experimental spectra as a weighted sum of the amorphous and crystalline phases. One can clearly see that a rapid crystallization is followed by a rather long postcrystallization “tail.”

fitted as a weighted sum of the initial (amorphous) and the final (well crystallized) states. One can see that up to the onset of crystallization, the structure remains unchanged (amorphous). This is followed by a rapid crystallization process (at ca. 160 °C) resulting in an abrupt increase of the fraction of the crystallized phase. Interestingly, the crystallization process has a rather long “tail” well above the crystallization temperature (up to 220 °C) when the degree of ordering in the material continues to increase, in agreement with the above idea. At the same time, the fact that there is no structural modification below the onset of crystallization demonstrates that changes in electrical conductivity in this temperature range are associated with thermal generation of charge carriers rather than with the structural modification of the material.

The existence of nonresonantly bonded Ge atoms is also manifested in the optical properties. In Fig. 8(a), we show simulated optical parameters for GeTe with different degrees of local disorder. To model the effect of increased local distortion upon the optical properties, we performed a series of density functional theory (DFT) calculations for the GeTe binary alloy studied earlier.<sup>11</sup> Previously, we have shown that a model containing 64 atoms, with Ge atoms randomly displaced along the pseudocubic  $\langle 111 \rangle$  directions such that Ge-Te distances are equal to 2.61 Å (the Ge-Te bond length in the amorphous

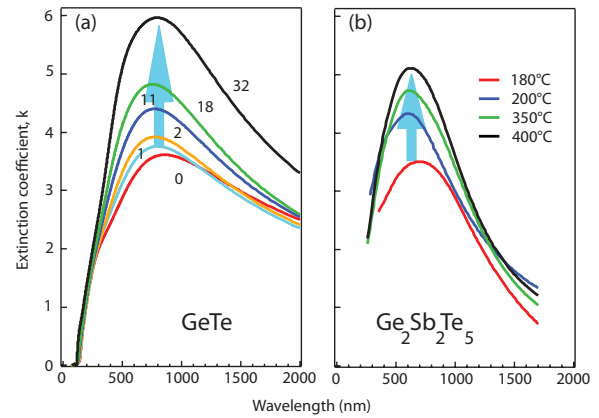


FIG. 8. (Color online) (a) Local disorder-induced variations of optical constants of GeTe; numbers indicate the numbers of resonantly bonded octahedral fragments. (b) Experimentally measured optical constants of  $\text{Ge}_2\text{Sb}_2\text{Te}_5$  as a function of annealing temperature. The direction of local order increase is indicated by arrows.

phase) with maximized atomic misalignment by randomly displacing tellurium atoms from their original crystallographic positions and thus disrupting the resonant bonding nature in the structure, was unstable and led to the spontaneous disintegration of crystalline GeTe into an amorphous state.<sup>11</sup> This state—which still retained the average cubic structure—was considered to be maximally disordered locally.

Assuming that the Te sublattice of GeTe is more stable and crystallization starts with the ordering of the Te sublattice (cf. Fig. 2), we gradually re-established the ordered structure by moving Te atoms back into the crystallographic positions of the GeTe crystalline phase. Since the extended  $p-p$  orbital interaction between the Ge and Te atoms requires a high degree of atomic alignment, the resonant bonding nature can be restored if all six Te atoms neighboring the same Ge atom occupy their proper crystallographic positions. We gradually moved Te atoms back to form one, two, four, etc., octahedrally bonded units and finally the equilibrium GeTe structure (32 octahedral units) was restored. As one can see, the extinction coefficient  $k$  gradually increases with an increase in the number of resonantly bonded octahedral sites.

Figure 8(b) shows experimentally measured values of  $k$  obtained through ellipsometry measurements for  $\text{Ge}_2\text{Sb}_2\text{Te}_5$  after annealing at different temperatures above the crystallization temperature. We have chosen  $\text{Ge}_2\text{Sb}_2\text{Te}_5$  for the experimental measurements because the range of property change upon annealing above the crystallization temperature is larger for this material than for GeTe (Ref. 9). As can be seen,  $k$  increases with increasing annealing temperatures, i.e., with an increase in local order. This result is in agreement with the published data obtained by others<sup>22</sup> as well as with the simulations shown in Fig. 8(a) and demonstrates a strong effect of the degree of local order on optical properties which is also in line with the results obtained in Ref. 23.

#### IV. CONCLUSIONS

In summary, our results show that the cubic rock-salt-like phase of GeTe-based phase-change alloys is intrinsically disordered from a bonding nature perspective and contains a

large fraction of nonresonantly bonded fragments. Their presence has a drastic effect on electronic properties. The present results suggest that the doping-related loss of coherency among local rhombohedral displacements<sup>5,6,8</sup> may serve as a means

to control the electrical properties of Ge-Sb-Te alloys. The experimentally observed decrease in the conductivity of GeTe and Ge<sub>2</sub>Sb<sub>2</sub>Te<sub>5</sub> upon doping by nitrogen<sup>24</sup> is in line with this hypothesis.

---

\*a.kolobov@aist.go.jp

<sup>1</sup>*Phase Change Materials: Science and Applications*, edited by S. Raoux and M. Wuttig (Springer-Verlag, New York, 2008).

<sup>2</sup>N. Yamada and T. Matsunaga, *J. Appl. Phys.* **88**, 7020 (2000).

<sup>3</sup>A. Kolobov, P. Fons, A. Frenkel, A. Ankudinov, J. Tominaga, and T. Uruga, *Nat. Mater.* **3**, 703 (2004).

<sup>4</sup>T. Chattopadhyay, J. Boucherle, and H. Von Schnering, *J. Phys. C* **20**, 1431 (1987).

<sup>5</sup>P. Fons, A. V. Kolobov, M. Krbal, J. Tominaga, K. S. Andrikopoulos, S. N. Yannopoulos, G. A. Voyiatzis, and T. Uruga, *Phys. Rev. B* **82**, 155209 (2010).

<sup>6</sup>T. Matsunaga, P. Fons, A. V. Kolobov, J. Tominaga, and N. Yamada, *Appl. Phys. Lett.* **99**, 231907 (2011).

<sup>7</sup>T. Matsunaga, H. Morita, R. Kojima, N. Yamada, K. Kifune, Y. Kubota, Y. Tabata, J.-J. Kim, M. Kobata, E. Ikenaga *et al.*, *J. Appl. Phys.* **103**, 093511 (2008).

<sup>8</sup>X. Biquard, M. Krbal, A. V. Kolobov, P. Fons, R. E. Simpson, B. Hyot, B. André, J. Tominaga, and T. Uruga, *Appl. Phys. Lett.* **98**, 231907 (2011).

<sup>9</sup>T. Siegrist, P. Jost, H. Volker, M. Woda, P. Merkelbach, C. Schlockermann, and M. Wuttig, *Nat. Mater.* **10**, 202 (2011).

<sup>10</sup>K. Shportko, S. Kremers, M. Woda, D. Lencer, J. Robertson, and M. Wuttig, *Nat. Mater.* **7**, 653 (2008).

<sup>11</sup>A. V. Kolobov, M. Krbal, P. Fons, J. Tominaga, and T. Uruga, *Nat. Chem.* **3**, 311 (2011).

<sup>12</sup>M. Krbal, A. V. Kolobov, P. Fons, J. Tominaga, S. R. Elliott, J. Hegedus, and T. Uruga, *Phys. Rev. B* **83**, 054203 (2011).

<sup>13</sup>G. C. Sosso, S. Caravati, R. Mazzarello, and M. Bernasconi, *Phys. Rev. B* **83**, 134201 (2011).

<sup>14</sup>G. Smolentsev, A. V. Soldatov, and M. C. Feiters, *Phys. Rev. B* **75**, 144106 (2007).

<sup>15</sup>F. Katmis, R. Calarco, K. Perumal, P. Rodenbach, A. Giussani, M. Hanke, A. Proessdorf, A. Trampert, F. Grosse, R. Shayduk *et al.*, *Cryst. Growth Des.* **11**, 4606 (2011).

<sup>16</sup>J. Hegedüs and S. Elliott, *Nat. Mater.* **7**, 399 (2008).

<sup>17</sup>S. Caravati, M. Bernasconi, T. D. Kuhne, M. Krack, and M. Parrinello, *Phys. Rev. Lett.* **102**, 205502 (2009).

<sup>18</sup>W. Welnic, A. Pamungkas, R. Detemple, C. Steimer, S. Blugel, and M. Wuttig, *Nat. Mater.* **5**, 56 (2005).

<sup>19</sup>X. Q. Liu, X. B. Li, L. Zhang, Y. Q. Cheng, Z. G. Yan, M. Xu, X. D. Han, S. B. Zhang, Z. Zhang, and E. Ma, *Phys. Rev. Lett.* **106**, 025501 (2011).

<sup>20</sup>R. Zallen, *The Physics of Amorphous Solids* (Wiley-VCH, Weinheim, Germany, 2004).

<sup>21</sup>S. Foulger, *J. Appl. Polym. Sci.* **72**, 1573 (1999).

<sup>22</sup>Y. K. Seo, J.-S. Chung, Y. S. Lee, E. J. Choi, and B. Cheong, *Thin Solid Films* **520**, 3458 (2012).

<sup>23</sup>B. Huang and J. Robertson, *Phys. Rev. B* **81**, 081204(R) (2010).

<sup>24</sup>S. Privitera, E. Rimini, and R. Zonca, *Appl. Phys. Lett.* **85**, 3044 (2004).